Manufacturing Rev. **9**, 17 (2022)

https://doi.org/10.1051/mfreview/2022013

Manufacturing Review
Available online at:
https://mfr.edp-open.org

RESEARCH ARTICLE OPEN ACCESS

A new environment-friendly magnetorheological finishing and fuzzy grey relation analysis in Ti-6Al-4V alloy polishing

Nguyen Trinh Duy, Dung Hoang Tien*, and Pham Thi Thieu Thoa

Faculty of Mechanical Engineering, Hanoi University of Industry, 298 Cau Dien, Bac Tu Liem District, Ha Noi, Vietnam

Received: 5 January 2022 / Accepted: 8 May 2022

Abstract. In this study, a naturally sourced cutting oil mixture using for the magnetorheological finishing (MRF) as an environmentally friendly carrier liquid. In addition, fuzzy grey relation analysis has been developed to predict and give optimal cutting parameters, the main factors affecting surface quality and material removal rate (MRR) identified. Experimental polishing procedures Ti-6Al-4V alloy were performed to confirm the availability of MRF models of the surface quality and MRR proposed. The fuzzy grey levels of elements to the polishing surface quality, namely the workpiece speed (n_w), working distances (K), MRF carrier speed (n_{MRF}) and feed rate (F), were 0.6983, 0.8057, 0.7818, and 0.7817, respectively. The analysis showed that the working distances (K) showed the most remarkable influence on the polishing effect, while the effect of workpiece speed (n_w) was the least important. Microscopic observations significantly minimize scratches on the surface. This observation provides an excellent reference value for high surface quality and material removal rate when polishing Ti-6Al-4V alloys.

Keywords: Magnetorheological finishing / FGRA / polishing / surface roughness / eco-friendly / Ti-6Al-4V alloy

1 Introduction

Ti-6Al-4V alloy has a melting point and excellent wear resistance, therefore widely used in industry [1–3]. With inherent mechanical and chemical properties of Ti-6Al-4V alloys, such as ductility, high adhesion ability, and excellent corrosion resistance, Ti-6Al-4V alloys are classified as the most challenging machining material [4–6]. Therefore, to meet the increasingly stringent requirements from the industries, the finishing process for Ti-6Al-4V alloy machining workpiece super-gloss poses a significant challenge for manufacturers and technicians. Traditional surface finishing techniques such as grinding have improved machining accuracy and surface finish. However, Ti-6Al-4V titanium alloy has poor grinding properties, low surface quality, and fast grinding wheel wear, which increases costs and low efficiency compared with other material grinding methods [7,8]. Therefore, to produce a super-glossy surface with very high precision, a non-traditional surface finishing process is required. The polishing under the support of magnetic fields is emerging as the advanced finishing method for high-gloss and precision finishes.

Magnetorheological finishing (MRF) forms by mixing a carbonyl iron particle (CIP) and abrasive particle (AP) with a carrier liquid to form a flexible polishing tool [9–11]. The MRF polishing tool works like Newton liquid in the absence of a magnetic field. Under the influence of the magnetic field, MRF immediately changes viscosity to a semi-solid state (non-Newton liquid). This process forms by the interaction between magnetic particles that arrange themselves according to the magnetic field lines and form a chain structure when a magnetic field is applied. The chain structure exhibits resistance to deformation when involved in removing residual materials under different machining modes. The studies reviewed by [12,13] show the feasibility and effectiveness of MRF polishing with various materials such as copper, ceramic, stainless steel, etc. and other geometrical shapes. Each other consists of flat discs, cylindrical tubes, free surfaces, etc. Amnieh et al. [14] developed a new MRF polishing device to complete the inner spiral grooves of a cylindrical aluminium tube with 70% improved surface roughness. To enhance the MRF polishing process, Barman et al. [15] have proposed MRF liquid mixed with nano abrasive particles as the polishing medium to perform the polishing process for the high surface quality bio-titanium alloy. Parameswari et al. [16] experimental study on a Ti-6Al-4V flat disk given the primary quality performance of the MRF process in achieving a mirror surface with the minimum

* e-mail: tiendung@haui.edu.vn

surface roughness of 95 nm. Initial surface roughness considering a vital treatment parameter, significantly affecting polishing efficiency.

The MRF components used in Luo et al. [17] study mainly contains four parts: CIP, AP, additive agents and deionized water. The active additive consists of a dispersion stabilizer and $NaCO_3$, respectively. The dispersion stabilizer contributes to the particles dispersing in the MRF suspension system with a pH value of the solution of 10. The studies reviewed by [18] also showed that to increase stability and flexibility of the polishing processes by MRF, the carrier fluids in the MRF mixture often have acidic or alkaline properties, thereby negatively impacting the operator's health as well as the environment. In addition, CIPs in this environment rapidly oxidize, especially when humidity and temperatures are high. When the CIPs are oxidized will directly affect MRF behaviour during polishing because iron oxides have inferior magnetic properties to pure iron. The studies of Foister et al. [19] showed that MRF with oxidized magnetic particles showed a 20% reduction in the magnetic effect under the influence of external magnetic fields. To solve this problem, Guo et al. [20] prepared an alternative MRF mixture in which ZrO_2 coated CIPs replace the pure CIPs. This new method has been successfully used to smooth the machining surface without leaving scratches or adhesion on the machining surface. However, the ZrO_2 coated CIPs are still in the development stage and have not been applied in different industries, with the cost of ZrO_2 coating being very high.

The biodegradability of the carrier fluids in MRFs is of equal importance to their use in polishing applications. It depends mainly on the carrier medium used in the fluid synthesis. Silicon oil, mineral oil, hydrocarbon oil, deionized water, etc., are commonly used carrier fluids. Of these carrier fluids, only deionized water is the biodegradable medium. However, it does not provide a good enough suspension for micrometre-sized CIPs and the AP, which leads to their rapid deposition. Furthermore, to increase the magnetism in the carrier liquid, deionized water components are often in an acidic or alkaline medium. Consequently, CIP particles corrode and oxidize over time resulting in reduced magnetism and yield stress of liquid structures. Deionized water-based carrier fluids cannot maintain the high temperature obtained during finishing. To overcome these problems, unique methods are implemented, such as adding additives to reduce sedimentation and enhance thermal stability, creating a coating for magnetic particles aim to avoid corrosion and improve the carrier liquid, etc. However, it increases the cost of the synthetic liquid. Combining the above problems with biodegradation, finding an environmentally friendly alternative carrier liquid is essential and overcoming the disadvantages mentioned above of deionized water. In this study, miscible oil metal cutting fluid is the best choice for heat removal, alternative maintenance restriction, antioxidant, and wear resistance cleaning chosen as the carrier liquid in polishing Ti-6Al-4V alloy. The cutting liquid is suitable for mixing with water and can be produced from vegetable oil and naphthenic oil. However, naphthenic oil is decreasing because of the concentration of additives compared to vegetable oils. This is considered very important, especially concerning environmental health and safety.

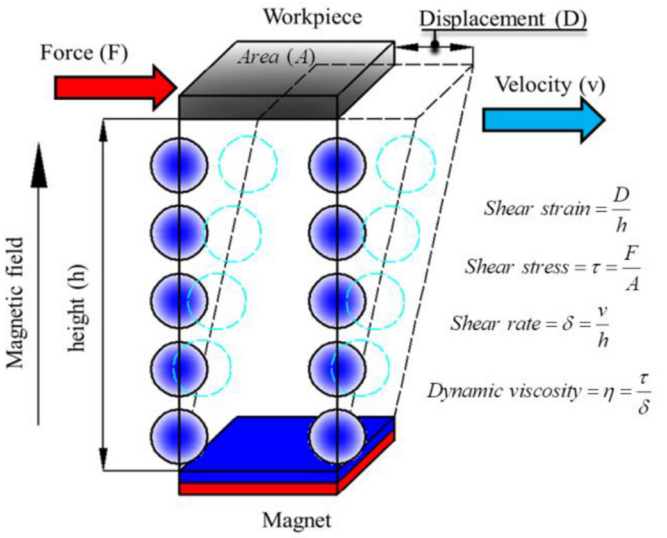

Fig. 1. MRF is mechanically deformed during polishing when a magnetic field is applied.

The fuzzy grey relationship analysis (FGRA) model considers all the different criteria, implies uncertainty in the weights of the criteria, and demonstrates the importance of the criteria by approaching a fuzzy system based on FGRA coefficient and FGRA level [21–23]. FGRA is an effective statistical method to measure the level of influence between the factors affecting the monitoring object. This method is very suitable for solving problems of incomplete information, little input data or lots of data but sporadic, uncertain and inconsistent. The FGRA method is used in many different fields, in which many researchers have optimized the processing parameters. The grey relation level indicates the degree of similarity between the comparison sequence and the reference sequence [24].

From the above characteristics, the authors have introduced a new polishing method with MRF containing inexpensive CIPs and Aps. The carrier liquid is a safe and eco-friendly cutting oil solution combined with a new hybrid algorithm for a super precise mirror polishing surface. In this work, after describing the principles and operating principles of MRF and the experiments were established. Experimental processes according to Taguchi L16 were performed to polish the Ti-6Al-4V surface. FGRA analyzed the experimental results to determine the different technological factors affecting the surface quality and the MRR, thereby giving the factors that have the most impact on these factors. The proposed method provides excellent reference values to improve the surface quality and MRR capability further.

2 Principle of operation and polishing MRF

2.1 Operation principle MRF

MRF is made from a suspension of micrometer-sized (about 20–50 μm) magnetized particles in the carrier liquid, with a

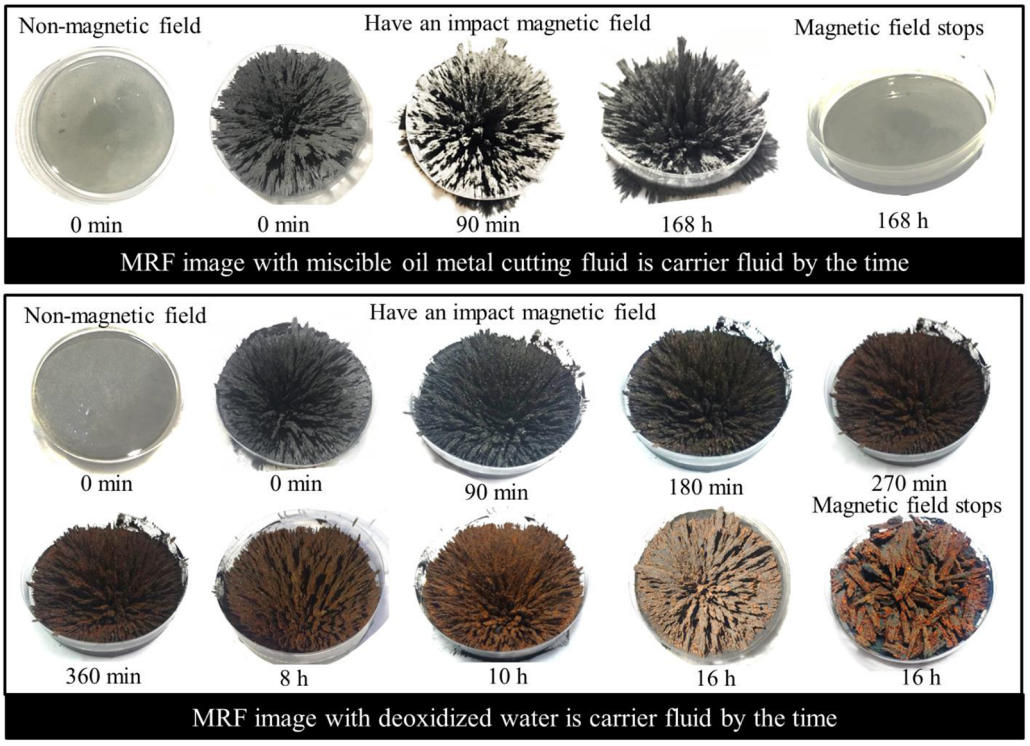

Fig. 2. Morphology of MRFs with different carrying fluids by the time.

magnetization particle volume percentage of 30–40%. A vital feature of the MRF is its ability to change its rheological behaviour quickly. When unaffected by a magnetic field, the liquid behaves like a normal liquid with properties close to those of the carrier liquid from which it is made. Under the action of a magnetic field, MRF acts as a semi-solid function of field strength. The magnetic field is inactive, and then MRF behaves like a carrier liquid again [25].

When there is an impact magnetic field, MRF is influenced by a magnetic field. It is mechanically deformed when participating in the polishing process, as shown in Figure 1. The inductive chains in the MRF obstruct the movements, thereby determining the flow behaviour change and polishability of the MRF. In general, there is an interaction between particles during polishing by MRF. This process creates friction, which contributes to the overall cutting stress and contributes to the smoothness of the workpiece surfaces. Therefore, it is essential to consider this effect when designing MRF and based devices MRF [26]. The friction depends on the viscosity of the carrier liquid. In the case of low viscosity, the friction is constant and non-magnetic particles are easily entrained into the space of the MRF system. At high viscosity, non-magnetic abrasive particles tend to move away from the contact area of magnetic particles [27]. This is demonstrated during polishing by MRF. When the carrier liquid has a higher viscosity than the working surface, more APs appear. However, when the viscosity is too large with the high polishing speed, it is easy to knock the APs off the polishing surface due to centrifugal force [28].

The CIPs in MRF with deionized water in nature are easily oxidized and dehydrated. Depending on the working conditions, particles can deteriorate quickly or slowly with time, humidity and temperature. Magnetic particle oxidation directly affects MRF behaviour in practical applications because iron oxides have inferior magnetic properties compared to pure iron. Under the influence of an external magnetic field, MRF with oxidized magnetic particles showed a 20% decrease in magnetic effect [24]. Figure 2 shows that the MRF with the proposed carrier solution has a high viscosity and excellent oxidation resistance, with almost no oxidation over time. The MRF returns to its original solution state when not affected by an active magnetic field. While the MRF from demagnetized water proposed by previous works [18,19] rapidly oxidizes, with water loss reducing viscosity, thus reducing polishability.

2.2 Polishing principles and experimental setting with MRF

The main experiment equipment includes a milling machine, magnet, jig, surface roughness measuring device, electronic scales, MRF carrier as shown in Figure 3. The workpiece is mounted on the main shaft of the milling machine via a jig and has a rotating speed of n_1. The permanent magnet is placed on the MRF carrier by material SUS 304 and mounted on the transmission box of motor 2. The direction of rotation of the MRF carrier is opposite to that of the milling machine spindle. The working distance K from the magnet surface to the

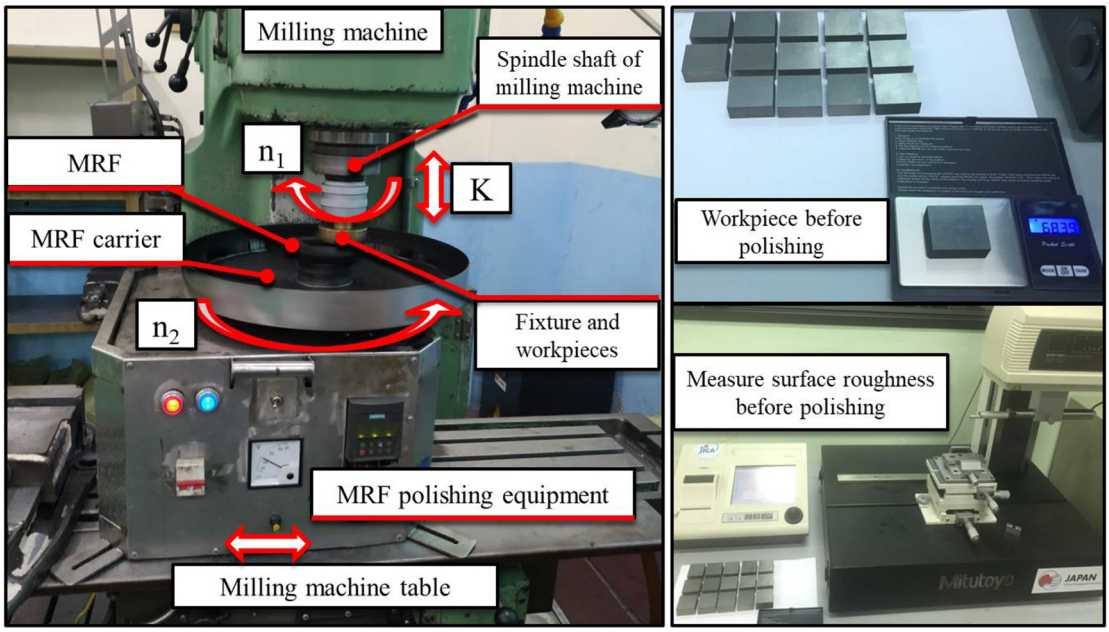

Fig. 3. MRF experimental equipment.

Table 1. Material parameters used in Ti-6Al-4V alloy polishing.

Mumerical order	Description	Material	Size	Relative magnetic permeability	Magnitude (A/m)
1	Permanent magnets	Nd-Fe	100 × 80 × 30 mm	1.09966	−890000
2	MRF carrier	SUS 304		1	
3	Polishing tool	MRF		5	
4	Workpiece	Ti-6Al-4V	32 × 32 × 20 mm	1	

workpiece surface can be adjusted by moving the milling machine table up or down. The polishing device is located on the milling machine table to create horizontal tooling movement when polishing. At this point, the polishing settings by MRF have been formed.

When K polishing distance is set, magnetic particles move in chains along the magnetic induction lines under the action of a magnetic field. Non-magnetic abrasive particles are affected by gravity and are exerted by a pulling force [28]. Under the combined action of these two force components, most of the non-magnetic APs in the MRF move onto the machining surface while exerting an exert force on the workpiece surface during machining. When the motor transmits rotational motion to the MRF at the speed of n_2, then the rotational movements are transmitted to the APs. Under the friction created between the workpiece and the APs, the micrometre size APs will take away a minimal amount of machining residual. The MRF should be set up directly above the permanent magnet to increase the polishing force between the APs and the workpiece [24]. The magnetic system comprises permanent magnets made of N50 type NdFeB material.

The workpiece materials and components used in MRF polishing are described in Table 1. The MRF sample preparation parameters are shown in Table 2, in which miscible oil with vegetable ester based cutting fluid manufactured by Vasco Jemtech Advanced Fluid Management, the CIPs with particle size 20–30 μm from manufacturer Henan Yuhuang Powder Metallurgy Plant, the APs used from Al_2O_3 with particle size of 30 μm is produced by Dengfeng Hongsheng Abrasives. Factors investigated during MRF polishing, including workpiece speed, working distance K, MRF carrier speed and feed rate, are shown in Table 3.

Along with increasing environmental awareness, today's machining process studies strive to exploit environmental safety features while preserving machining properties such as having a high viscosity index, good viscosity at high temperature, good abrasion resistance, and high flash point, low volatility, non-toxic, easy to biodegradable, etc. Studies of [29] for a vegetable oil-based water-soluble cutting liquid have solved the above requirements. On that basis, the percentage components by weight of the cutaneous liquid are described in Table 4.

Table 2. MRF components.

Mumerical order	Description	Particles size	Percentage of components in the MRF	Magnetic permeability (N/A^2)	Magnetic sensitivity	Specific weight (kg/cm^3)
1	CIP	20–30 μm	40%	$\mu = 5.03 \times 10^{-4}$	$\times_m = 10^3$	$\rho_C = 7.8 \times 10^{-3}$
2	AP	30 μm	12%		$\times'_m = 10^3$	$\rho_A = 3.965 \times 10^{-3}$
3	Miscible oil cutting fluid		45%			$\rho_A = 0.9187 \times 10^{-3}$
4	α-cellulose		3%			

Table 3. Parameter level of MRF polishing technology according to Taguchi method.

Level	Workpiece speed (n_w) (rpm)	Working distances (K) (mm)	MRF carrier speed (n_{MRF}) (rpm)	Feed rate (F) (mm/min)
1	530	1	25	250
2	720	1.25	30	500
3	980	1.5	35	750
4	1330	1.75	40	900

Table 4. Components by weight of miscible water cutting fluid based vegetable oils [30].

Mumerical order	Material	Percentage (%)	Mumerical order	Material	Percentage (%)
1	Vegetable oils	5–20	6	Anti-rust agents	0–3
2	Synthetic esters of vegetable oils	15–35	7	Extreme pressure agents	0–3
3	Waters	5–15	8	Aseptic	0–2
4	Emulsifying agents	2–12	9	Defoamer	0–2
5	Dispersing agents	0–2	10	Alkaline reserve	15–30

Table 5. Experimental procedure by Taguchi L16 method.

Experiments order	Factor and level				MRR (mg/min)	Average surface roughness value Ra_m (μm)
	Workpiece speed (n_w)	MRF carrier speed (n_{MRF})	Feed rate (F)	Working distance *(K)*		
1	1	1	1	1	13.33	0.041
2	1	2	2	2	11.66	0.059
3	1	3	3	3	10	0.089
4	1	4	4	4	7.67	0.098
5	2	1	2	3	14.15	0.044
6	2	2	1	4	12.83	0.050
7	2	3	4	1	10.50	0.057
8	2	4	3	2	9.21	0.079
9	3	1	3	4	15.30	0.067
10	3	2	4	3	13.26	0.080
11	3	3	1	2	10.83	0.081
12	3	4	2	1	9.33	0.091
13	4	1	4	2	15.92	0.040
14	4	2	3	1	14.02	0.059
15	4	3	2	4	11.17	0.062
16	4	4	1	3	9.60	0.071

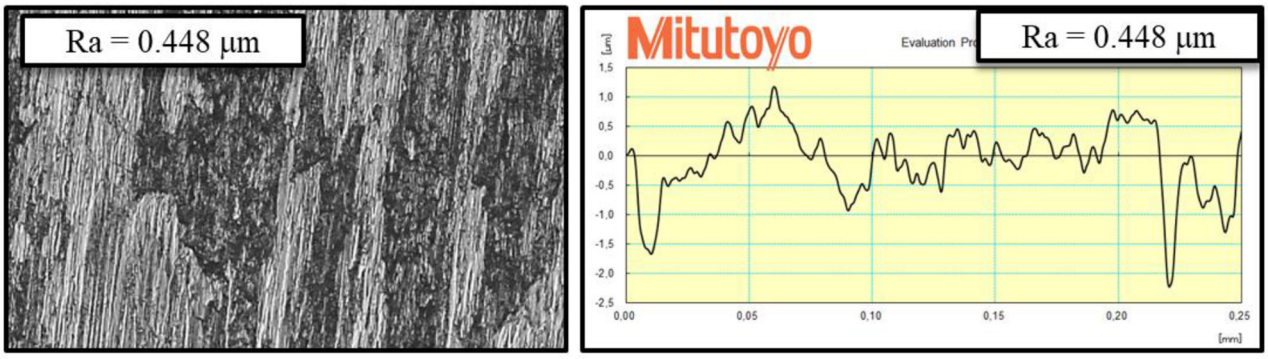

Fig. 4. SEM surface and roughness profile of workpiece before polishing.

The Taguchi experimental design is a method commonly used to investigate the impact factors, including many factors and levels [29]. This method has been successfully applied to many different fields to save many experiments and time from getting the optimal target group [30]. The key to this approach is to create an orthogonal design table based on the investigated factors and impact levels. In this work, the MRF polishing experiments for Ti-6Al-4V titanium alloy were set up according to the Taguchi experimental design [30], as shown in Table 5. Before being polished, workpieces grinding on a single crystal diamond grinding wheel, giving a surface roughness of about $Ra = 0.42$ μm. This work aims to obtain parameters for the polishing process to create an ultra-precise mirror surface with the difficult-to-work material (Ti-6Al-4V alloy).

The workpieces are cleaned with acetone and ethanol and then dried before polishing. The workpieces were weighed before and after polishing with a high-resolution electronic balance (0.1 mg) to determine MRR. In this case, the MRR is determined by the following equation:

$$\text{MRR} = \frac{\Delta m \times 10^3}{T} \quad (1)$$

where Δm (g) is the difference between the workpiece weight before and after polishing, T (min) is polishing time and MRR (mg/min) is material removal rate.

The surface roughness obtained after polishing is measured on the Mitutoyo SJ201 roughness tester. The roughness value obtained is the average of three measurements at different positions on the same surface. The workpiece surface shape after polishing is observed with an electron microscope.

3 Results and discussion

Figures 4 and 5 show the SEM and surface roughness before and after polishing with different technological parameters. The polishing experiments yield surfaces with a high gloss and precision from the original rough surface. Scratches left by a previous grinding operation have been significantly improved and reduced. For further investigation, the surface quality after polishing, as described in Figure 5, shows that surfaces are obtained from electron microscopy after 90 minutes of polishing. The experimental procedure was conducted according to the Taguchi L16 method with workpiece speed (n_w), MRF carrier speed (n_{MRF}), feed rate (F) and working distance (K).

The polishing experiments with MRF performed by Parameswari et al. [16] apply to the polishing process of Ti-6Al-4V alloy from grinding surfaces with an average surface roughness $Ra = 0.415$ mm. After polishing by Parameswari et al. [16], results showed that the best surface quality was obtained with $Ra = 94$ nm (0.094 μm). As described in Figure 6, our experimental results show that the surface quality from the proposed method is significantly improved compared to before polishing. The experimental processes corresponding to different polishing technology modes will have different MRR and surface quality. However, it can be seen that the surface quality obtained from our experiments is significantly improved compared to the method proposed by Parameswari et al. [16]. Our study resulted in the best surface quality corresponding to $Ra = 40$ nm, and the surface quality improved by 57.44% compared with the proposed method by Parameswari et al. [16].

Figure 6 shows the surface roughness parameters before and after polishing. The initial grinding surfaces ($Ra \approx 0.35$ μm) are significantly improved with $Ra < 0.1$ μm under different test conditions. The highest gloss surface was obtained by experiment 13 with polishing distance $K = 1$ mm machining conditions, workpiece speed 1330 rpm, MRF carrier speed 40 rpm and feed rate $F = 500$ mm/min, the mirror surface $Ra = 0.040$ μm is obtained after this polishing process. With experiment 4, polishing distance $K = 1.75$ mm, spindle speed 530 rpm, MRF carrier speed 40 rpm, and feed rate $F = 900$ mm/min, for maximum roughness, the mirror surface $Ra = 0.098$ μm after this polishing process. Experimental procedures showed different surface qualities produced by different technological parameters when polishing Ti-6Al-4V alloy. However, the polishing surfaces are all mirror-like, thereby demonstrating the effectiveness of the proposed polishing method.

To determine the influence of technological factors such as workpiece speed, polishing distance, MRF carrier speed and feed rate to Ra and MRR. The FGRA coefficients are applied to determine the main factors that affect the

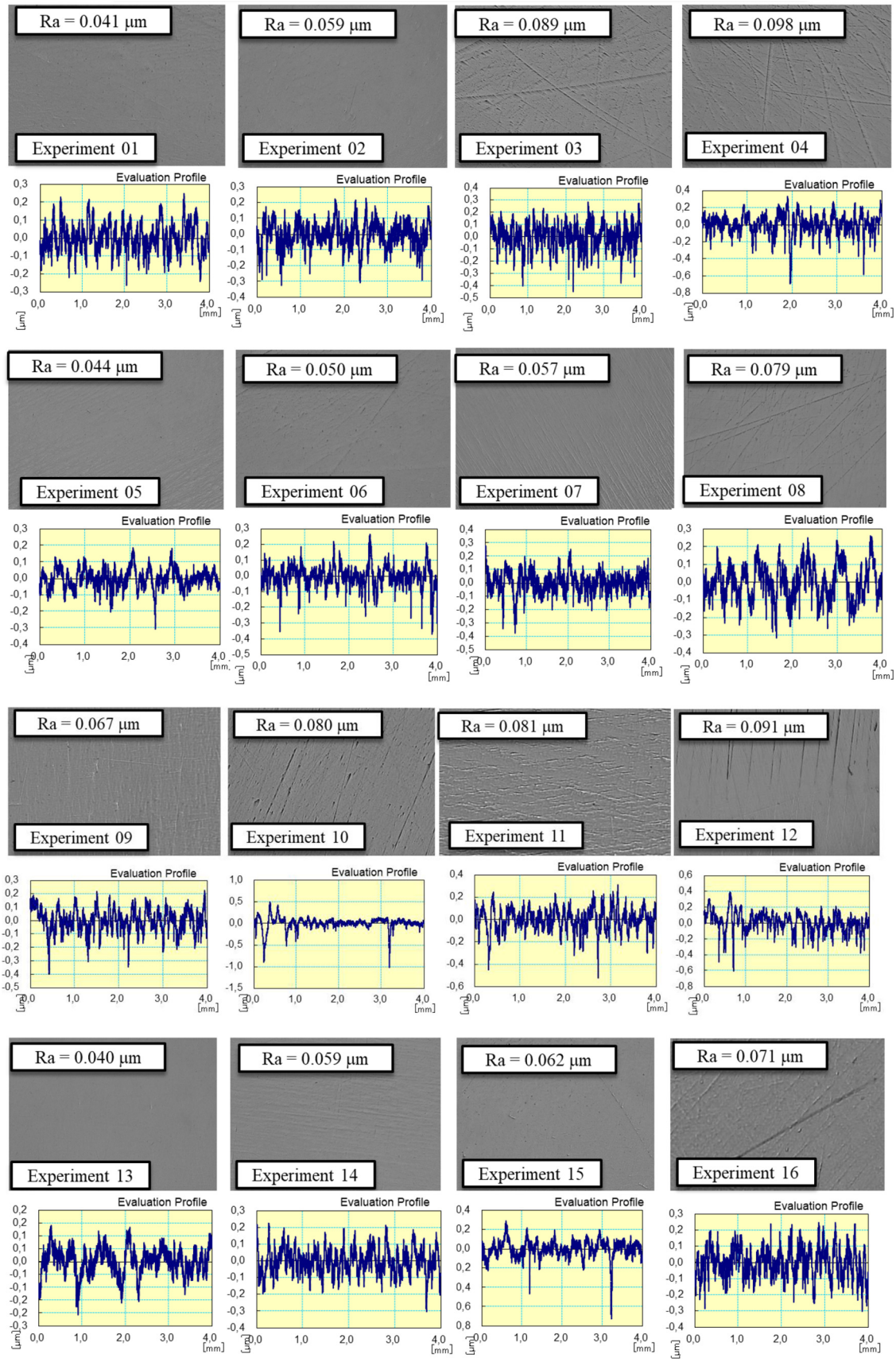

Fig. 5. SEM and roughness image of workpiece surface after polishing Ti-6Al-4V under different experimental conditions.

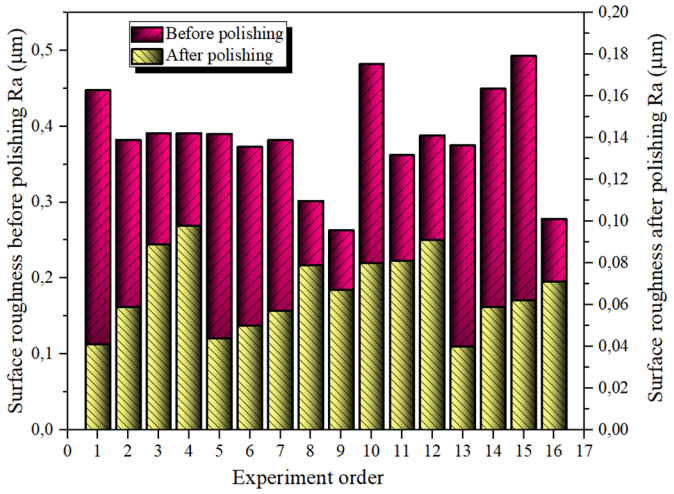

Fig. 6. Surface roughness of workpiece before and after 90 minutes polishing under different test conditions.

quality of the polished surface and MRR. The comparison and reference matrices are handled as follows:

See equations (2),(3) below.

Figures 7 and 8 illustrate the fuzzy membership classes of the four technological factors that affect polishability through the output parameters *Ra* and MRR. The fuzzy membership layers of the factors that affect the polishing process differ significantly.

The fuzzy member layer results analysis showed that with MRR, the change in workpiece speed was kept at the highest level (0.7654), then the MRF carrier speed (0.7148) and feed rate (0.6982). Meanwhile, the working distance has the lowest value (0.6185). Analysis results with *Ra* showed a significant difference compared with MRR. The workpiece speed change is kept at the lowest level (0.5921), followed by the MRF carrier speed (0.7383) and the feed rate (0.7487), with the change of polishing distance K valid the largest (0.7805). Thus, the influence of polishing distance K affects the surface quality most when polishing. Meanwhile, the workpiece speed has the lowest impact on the polishing surface quality. However, when surveyed with MRR tends to be opposite to *Ra*. The workpiece speed has the most significant effect, while the working distance K has the most negligible influence on MRR.

As shown in Figures 7 and 8, the fuzzy Euclidean relation layer of the four elements in the polishing process shows negligible differences. However, it still shows that with MRR, the fuzzy Euclidean relation layer of the

$$\begin{bmatrix} Y_1(x) & & & & & & & & & & & & & & & \\ Y_2(x) & & & & & & & & & & & & & & & \\ Y_3(x) & & & & & & & & & & & & & & & \\ Y_4(x) & & & & & & & & & & & & & & & \\ & & & & & & & Y(x) & & & & & & & & & \end{bmatrix}$$
$$= \begin{bmatrix} 530 & 530 & 530 & 530 & 720 & 720 & 720 & 720 & 980 & 980 & 980 & 980 & 1330 & 1330 & 1330 & 1330 \\ 1 & 1,25 & 1,50 & 1,75 & 1 & 1,25 & 1,50 & 1,75 & 1 & 1,25 & 1,50 & 1,75 & 1 & 1,25 & 1,50 & 1,75 \\ 25 & 30 & 35 & 40 & 30 & 25 & 40 & 35 & 35 & 40 & 25 & 30 & 40 & 35 & 30 & 25 \\ 250 & 500 & 750 & 900 & 750 & 900 & 250 & 500 & 750 & 900 & 500 & 250 & 500 & 250 & 900 & 750 \\ 13,33 & 11,66 & 10 & 7,67 & 14,15 & 12,83 & 10,50 & 9,21 & 15,30 & 13,26 & 10,83 & 9,33 & 15,92 & 14,02 & 11,17 & 9,60 \end{bmatrix} \quad (2)$$

$$\begin{bmatrix} Z_1(x) & & & & & & & & & & & & & & & \\ Z_2(x) & & & & & & & & & & & & & & & \\ Z_3(x) & & & & & & & & & & & & & & & \\ Z_4(x) & & & & & & & & & & & & & & & \\ & & & & & & & Z(x) & & & & & & & & & \end{bmatrix}$$
$$= \begin{bmatrix} 530 & 530 & 530 & 530 & 720 & 720 & 720 & 720 & 980 & 980 & 980 & 980 & 1330 & 1330 & 1330 & 1330 \\ 1 & 1,25 & 1,50 & 1,75 & 1 & 1,25 & 1,50 & 1,75 & 1 & 1,25 & 1,50 & 1,75 & 1 & 1,25 & 1,50 & 1,75 \\ 25 & 30 & 35 & 40 & 30 & 25 & 40 & 35 & 35 & 40 & 25 & 30 & 40 & 35 & 30 & 25 \\ 250 & 500 & 750 & 900 & 750 & 900 & 250 & 500 & 750 & 900 & 500 & 250 & 500 & 250 & 900 & 750 \\ 0,041 & 0,059 & 0,089 & 0,098 & 0,044 & 0,050 & 0,057 & 0,079 & 0,067 & 0,080 & 0,081 & 0,091 & 0,040 & 0,059 & 0,062 & 0,071 \end{bmatrix} \quad (3)$$

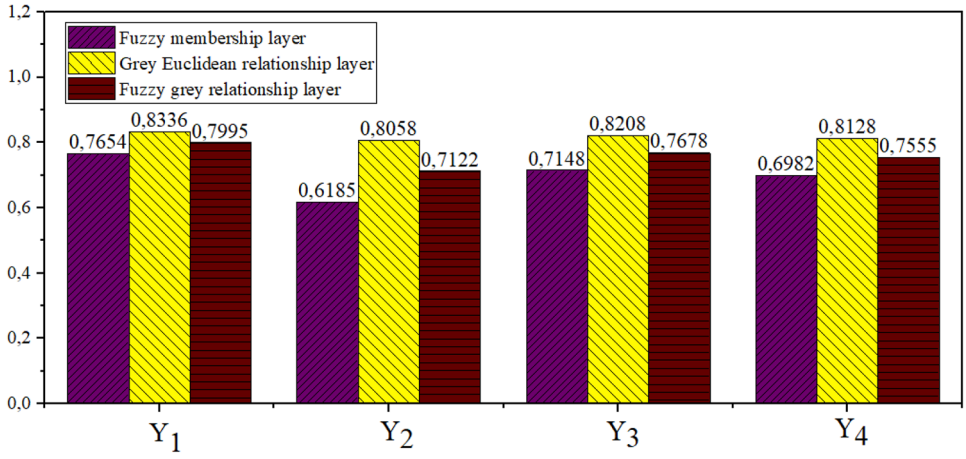

Fig. 7. The results analysis of the fuzzy grey relationship with MRR.

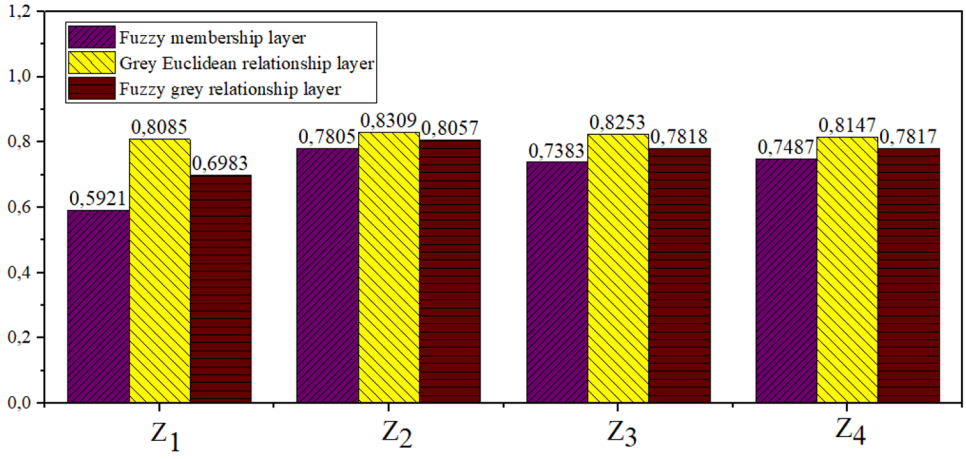

Fig. 8. The results analysis of the fuzzy grey relationship with *Ra*.

workpiece speed is highest, while with MRR, the fuzzy Euclidean relation layer of the working distance is the highest. Thus changing the working distance leads to better polishing surface quality than changing workpiece speed, MRF carrier speed and feed rate. Meanwhile, changing the workpiece has the most influence on MRR compared to changing the remaining parameters.

The fuzzy grey relationship layer of the four factors up to the surface polishability is shown in Figures 7 and 8. The analysis provides an overview to evaluate survey factors that affect the polished surface quality and MRR. The fuzzy grey relationship layer for the *Ra* of the four elements (workpiece speed, working distance, MRF carrier speed and feed rate) are 0.6983, 0.8057, 0.7818, and 0.7817. Meanwhile, the fuzzy grey relationship layer to the MRR of the four elements were 0.7995, 0.7122, 0.7678 and 0.7555. Therefore, the polishing for Ti-6Al-4V alloy shows that the working distance must first be chosen for high surface quality, while with MRR, the workpiece speed is the preferred choice.

4 Conclusions

This paper presents a polishing method with MRF based on miscible oil cutting fluid of natural origin. The advantage of the proposed MRF model has resulted in a polishing model associated with environmental protection, along with its outstanding antioxidant performance compared to MRFs of deionized water. In addition, the improved FGRA algorithm was applied to determine the technological parameters that have the most and the most negligible influence on the surface quality and material removal rate, thereby increasing the polishing efficiency. According to work done, the main conclusions are drawn as follows:

– Provides a polishing tool for challenging machining and expensive materials from low-cost and environmentally friendly materials. The polishing carrier liquid is established based on miscible oil cutting fluid of natural origin, low-cost CIPs and APs.

– A new MRF with the proposed carrier solution has a high viscosity and excellent oxidation resistance, with almost no oxidation over time. When not affected by an active magnetic field, the MRF returns to its original solution state.
– The polishing Ti-6Al-4V material yielded the fuzzy grey relationship layer for the Ra of the four elements (workpiece speed, working distance, MRF carrier speed and feed rate) are 0.6983, 0.8057, 0.7818, and 0.7817. Meanwhile, the fuzzy grey relationship layer to the MRR of the four elements were 0.7995, 0.7122, 0.7678 and 0.7555. Therefore, the polishing for Ti-6Al-4V alloy shows that the working distance must first be chosen for high surface quality, while with MRR, the workpiece speed is the preferred choice.
– The analysis results with the proposed MRF polishing model show that the superfine Ti-6Al-4V alloy surface can be produced with the surface roughness $Ra = 0.040$ μm according to the parameters $K = 1$ mm, $n_w = 1330$ rpm, $n_{MRF} = 40$ rpm and $F = 500$ mm/min. Hence the polishing process using MRF with inexpensive CIP and AP particles and vegetable oil carrier liquid can create an ultra-fine Ti-6Al-4V surface without affecting the environment and high efficiency.

Conflict of interest

The authors have nothing to disclose and no conflict of interests regarding the publication of this paper.

References

1. D. Nguyen et al., Online monitoring of surface roughness and grinding wheel wear when grinding Ti-6Al-4V titanium alloy using ANFIS-GPR hybrid algorithm and Taguchi analysis, Precis. Eng. **55** (2019) 275–292
2. Z. Tao et al., FE modeling of a complete warm-bending process for optimal design of heating stages for the forming of large-diameter thin-walled Ti–6Al–4V tubes, Manufactur. Rev. **4** (2017) 8
3. J.O. Obiko, F.M. Mwema, M.O. Bodunrin, Validation and optimization of cutting parameters for Ti-6Al-4V turning operation using DEFORM 3D simulations and Taguchi method, Manufactur. Rev. **8** (2021) 5
4. J. Ju et al., Evolution of the microstructure and optimization of the tensile properties of the Ti–6Al–4V alloy by selective laser melting and heat treatment, Mater. Sci. Eng. A **802** (2021) 140673
5. S.R. Oke et al., An overview of conventional and non-conventional techniques for machining of titanium alloys, Manufactur. Rev. **7** (2020) 34
6. V.V.K. Lakshmi et al., Parametric optimization while turning Ti-6Al-4V alloy in Mist-MQCL (Green environment) using the DEAR method, Manufactur. Rev. **7** (2020) 38
7. N. Qian et al., Axial rotating heat-pipe grinding wheel for eco–benign machining: a novel method for dry profile-grinding of Ti–6Al–4V alloy, J. Manufactur. Process. **56** (2020) 216–227
8. B. Zhao et al., Characterisation of the wear properties of a single-aggregated cubic boron nitride grain during Ti–6Al–4V alloy grinding, Wear 452-453 (2020) 203296
9. H. Luo et al., Optimized pre-thinning procedures of ion-beam thinning for TEM sample preparation by magnetorheological polishing, Ultramicroscopy **181** (2017) 165–172
10. L. Nagdeve, V.K. Jain, J. Ramkumar, Nanofinishing of freeform/sculptured surfaces: state-of-the-art, Manufactur. Rev. **5** (2018) 6
11. V. Kumar, R. Kumar, H. Kumar, Rheological characterization of vegetable-oil-based magnetorheological finishing fluid, Mater. Today **18** (2019) 3526–3531
12. M. Ashtiani, S.H. Hashemabadi, A. Ghaffari, A review on the magnetorheological fluid preparation and stabilization, J. Magn. Magn. Mater. **374** (2015) 716–730
13. A.K. Bastola, M. Hossain, A review on magneto-mechanical characterizations of magnetorheological elastomers, Compos. Part B: Eng. **200** (2020) 108348
14. M. Givi, A. Fadaei Tehrani, A. Mohammadi, Polishing of the aluminum sheets with magnetic abrasive finishing method, Int. J. Adv. Manufactur. Technol. **61** (2012) 989–998
15. H. Barman, S. Hegde, Comprehensive review of parameters influencing the performance of magnetorheological elastomers embedded in beams, Mater. Today **26** (2020) 2130–2135
16. G. Parameswari et al., Experimental investigations into nanofinishing of Ti6Al4V flat disc using magnetorheological finishing process, Int. J. Adv. Manufactur. Technol. **100** (2019) 1055–1065
17. H. Luo et al., An atomic-scale and high efficiency finishing method of zirconia ceramics by using magnetorheological finishing, Appl. Surf. Sci. **444** (2018) 569–577
18. C. Kumari, S.K. Chak, A review on magnetically assisted abrasive finishing and their critical process parameters, Manufactur. Rev. **5** (2018) 13
19. S. Rosenfeldt et al., Chapter 5 – Self-assembly of magnetic iron oxide nanoparticles into cuboidal superstructures, in Novel Magnetic Nanostructures, edited by N. Domracheva, M. Caporali, E. Rentschler (Elsevier, 2018), pp. 165–189
20. H. Guo et al., Effects of pressure and shear stress on material removal rate in ultra-fine polishing of optical glass with magnetic compound fluid slurry, J. Mater. Process. Technol. **214** (2014) 2759–2769
21. O.M. Olabanji, K. Mpofu, Appraisal of conceptual designs: coalescing fuzzy analytic hierarchy process (F-AHP) and fuzzy grey relational analysis (F-GRA), Res. Eng. **9** (2021) 100194
22. E. Jiaqiang et al., Heat dissipation investigation of the power lithium-ion battery module based on orthogonal experiment design and fuzzy grey relation analysis, Energy **211** (2020) 118596
23. P. Muthu, Multi objective optimization of wear behaviour of Aluminum MMCs using Grey-Taguchi method, Manufactur. Rev. **7** (2020) 16
24. A. Roozbahani, H. Ghased, M. Hashemy Shahedany, Inter-basin water transfer planning with grey COPRAS and fuzzy COPRAS techniques: a case study in Iranian Central Plateau, Sci. Total Environ. **726** (2020) 138499
25. H.K. Latha, P. Usha Sri, N. Seetharamaiah, Design and manufacturing aspects of magneto-rheological fluid (MRF) clutch, Mater. Today **4** (2017) 1525–1534
26. F. Wang et al., Rheological properties and sedimentation stability of magnetorheological fluid based on multi-walled

carbon nanotubes/cobalt ferrite nanocomposites, J. Mol. Liquids **324** (2021) 115103
27. A. Fakhar, R. Kolahchi, Dynamic buckling of magneto-rheological fluid integrated by visco-piezo-GPL reinforced plates, Int. J. Mech. Sci. **144** (2018) 788–799
28. J. Zheng et al., The induced field of magnetized wall on the static normal force of magnetorheological fluids, J. Magn. Magn. Mater. **504** (2020) 166652
29. A. Pal, S.S. Chatha, H.S. Sidhu, Experimental investigation on the performance of MQL drilling of AISI 321 stainless steel using nano-graphene enhanced vegetable-oil-based cutting fluid, Tribol. Int. **151** (2020) 106508
30. C.Y. Chan, W.B. Lee, H. Wang, Enhancement of surface finish using water-miscible nano-cutting fluid in ultra-precision turning, Int. J. Mach. Tools Manufact. **73** (2013) 62–70

Cite this article as: Nguyen Trinh Duy, Dung Hoang Tien, Pham Thi Thieu Thoa, A new environment-friendly magnetorheological finishing and fuzzy grey relation analysis in Ti-6Al-4V alloy polishing, Manufacturing Rev. **9**, 17 (2022)